*Pure & Appl. Chem.*, Vol. 50, pp. 759-769.
Pergamon Press Ltd.1978. Printed in Great Britain

0033-4545/78/0801-0759 $02.00/0

# APPLICATIONS OF LASERS IN CHEMICAL SPECTROSCOPY AND DYNAMICS: HIGHER ORDER SUSCEPTIBILITY EFFECTS

Robin M. Hochstrasser and G. R. Meredith

Department of Chemistry and Laboratory for Research on the Structure of Matter, University of Pennsylvania, Philadelphia, Pennsylvania 19104

Abstract - A survey of recent experiments on molecular excited states will be presented. Many non-linear optical processes have now become extremely useful in chemical spectroscopy and dynamics. Laser E-fields induce a dipole moment $\mu$ in molecular systems which in turn acts as a source of additional fields in the medium. The polarization is generally a power series in the fields:

$$N\mu = \chi^{(1)}E + \chi^{(2)}EE + \chi^{(3)}EEE + \ldots.$$

Normally, centrosymmetric molecules have $\chi^{(2)} = 0$ and systems that are centrosymmetric will not generally exhibit second harmonic generation. Thus the study of $\chi^{(2)}$ in such cases has provided information on the magnetically induced SHG. This effect coupled with the two-photon absorption, a resonant part of $\chi^{(3)}$, was used to explore polariton effects in molecular crystals of anthracene and naphthalene. High resolution spectroscopy of gases and solids were also accomplished using three wave mixing brought about through two-photon and Raman resonances in $\chi^{(3)}$. These techniques allow accurate measurements of two-photon cross-sections. The various non-linear experiments yield new information on the relaxation and dephasing dynamics in molecular excited states.
Pulsed lasers permit the resolution in time of excited state relaxation in the condensed phase and experiments will be described in which non-linear phenomena were used to study vibrational relaxation in some simple diatomic solids at low temperature, and chemical reactions in the condensed phase.

## 1. INTRODUCTION:

During the sixties Bloembergen and his coworkers developed the ground work of the field of non-linear optics (1) and now those concepts are beginning to have impact on chemistry. Primarily the new found importance of non-linear responses in systems of chemical interest arises because of the availability of high powered tunable lasers. The power is needed in order that the higher order terms in the expansion of the dipole moments of the constituents contribute significantly to the polarization of the system; the tunability is required in order that the effects of specific molecular resonances can be explored.

The dipole moment per unit volume, or polarization, of a collection of molecules, ions or radicals may be expressed as:

$$N\mu_\alpha = P_\alpha = \chi^{(1)}_{\alpha\beta} E_\beta + \chi^{(2)}_{\alpha\beta\gamma} E_\beta E_\gamma + \chi^{(3)}_{\alpha\beta\gamma\delta} E_\beta E_\gamma E_\delta + .. \qquad (1)$$

where the indices $\alpha$, $\beta$, .. represent space fixed axis designations (repeated indices are summed over) and $\chi^{(n)}_{\alpha\beta..}$ is the $\alpha\beta..$ component of the $n^{th}$- order susceptibility tensor.

The literature contains many discussions of the macroscopic and microscopic origin of these tensors (1 to 5). A main point is that the existence of $\chi^{(n)}_{\alpha\beta..}$ and the presence of optical and/or static fields $E_\beta$, $E_\gamma$.. implies the existence of a polarization $P_\alpha$. This polarization acts as a source term in generating a new optical field, the relations between

the polarization and the field being specified by the classical Maxwell's equations. Incoherent phenomena in the medium (e.g. fluorescence, phosphorescence, relaxations) occur only after the coherent polarization is damped. This article will be mainly concerned with measurements relating to the coherent effects and with the dissipative pathways or other types of scattering. The absorption of light corresponds to the formation of an incoherent population in which $N<\mu>$ is zero.

From the standpoint of spectroscopy it is important to recognize the effects of resonances on the various susceptibilities in equation (1). The purpose of the present paper is to describe some recent applications of non-linear optics to molecular spectroscopy and chemical dynamics. In each application a key feature will be that the process is resonance enhanced by a molecular transition. The relationship between the various induced spectroscopic processes and the susceptibility tensors in equation (1) is not really obvious. The chemical spectroscopist has usually been interested in the microscopic description of resonance phenomena in order that spectroscopic assignments may be used as a means of better understanding molecular structure. However the observed phenomena associated with the higher order susceptibilities require a more detailed consideration of the bulk material properties. If the susceptibilities are considered to be dipolar susceptibilities, in other words the various transition moments are all transition dipole moments, then important symmetry criteria can be readily deduced (5 and 6). For example $\chi^{(1)}$ exists for all materials regardless of their symmetry because it represents the constant of proportionality between two polar vectors ($\mu$ and E). The microscopic form of $\chi^{(1)}$, the usual polarizability, contains the transition dipole factor connecting the ground state (g) to and from all excited states (i), $\mu_{gi}\mu_{ig}$ and this factor exists for some i in all symmetry groups. The second-order susceptibility $\chi^{(2)}$ is clearly zero in centrosymmetric systems (suppose inversion through an origin transformed the system into itself, then the vector P would change sign, the product $E^2$ would remain unchanged so $\chi^{(2)}$ would equal $-\chi^{(2)}$) and this includes molecules belonging in centrosymmetric point groups, crystals in centrosymmetric space groups, as well as gases and liquids containing molecules of any symmetry. The observed coherent optical properties involve the square of the polarization. The absorption of energy is given by the cycle average $<P_\alpha E_\alpha>$. So it is easy to see that all incoherent non-linear properties (those dependent on a power of the light intensity greater than one must be described in the third or higher odd order susceptibility. The majority of the better known non-linear processes occur through $\chi^{(3)}$. The second order susceptibility while giving rise to frequency mixing (second harmonic generation, up and down conversion) does not describe absorption processes because $<\chi^{(2)} E_\alpha E_\beta E_\alpha> = 0$. Figure 1 summarizes the various processes that are discussed herein.

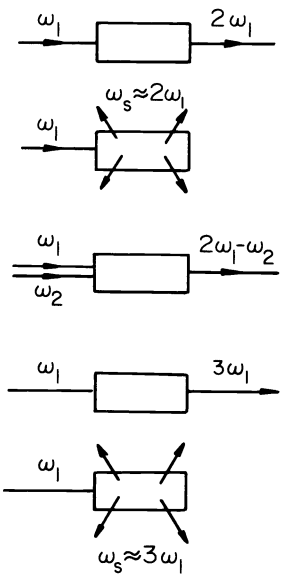


$\chi^{(2)}(-2\omega_1, \omega_1, \omega_1)$
SECOND HARMONIC GENERATION

$\mathrm{Im}\chi^{(3)}(-\omega_1, -\omega_1, \omega_1, \omega_1)$
TWO-PHOTON ABSORPTION

$\chi^{(3)}(\omega_2 - 2\omega_1, \omega_1, \omega_1, -\omega_2)$
CARS $\omega_1 - \omega_2 = \hbar\omega_v$
TWO-PHOTON RESONANCE $2\omega_1 = \hbar\omega_i$

$\chi^{(3)}(-3\omega_1, \omega_1, \omega_1, \omega_1)$
THIRD HARMONIC GENERATION

$\mathrm{Im}\chi^{(5)}(-\omega_1, -\omega_1, -\omega_1, \omega_1, \omega_1, \omega_1)$
THREE PHOTON ABSORPTION

Figure 1. Schematic of various coherent and incoherent non-linear processes.

## 2. RESONANCE ENHANCED SECOND HARMONIC GENERATION:

In second harmonic generation coherent light at $\omega_1$ is converted into coherent light at $2\omega_1$. Normally this process occurs only for non-centrosymmetric solids, liquids or gases (i.e. in the presence of applied electric fields in the case of isotropic systems). A number of molecular crystals are non-centrosymmetric and exhibit frequency doubling (4). The microscopic form for $\chi^{(2)}$ near a homogeneous resonance ($\omega_{oi} \approx \omega_1 + \omega_2$) is:

$$\frac{\varepsilon_3 \cdot \mu_{oi} / \hbar^2}{\omega_{io} - \omega_1 - \omega_2 + i\Gamma} \sum_j \left[ \frac{\varepsilon_1 \cdot \mu_{ij} \mu_{jo} \cdot \varepsilon_2}{\omega_{jo} - \omega_2} + \frac{\varepsilon_2 \cdot \mu_{ij} \cdot \mu_{jo} \cdot \varepsilon_1}{\omega_{jo} - \omega_1} \right] \tag{2}$$

The imaginary part or modulus squared of the first part is the one photon spectral profile of the $o \rightarrow i$ transition. The second term is a two-photon amplitude linking the ground state and the resonant state i. This amplitude is not sensitive in the usual case to small changes in the frequencies $\omega_1$ and $\omega_2$. The usual case is where $|i\rangle$ is a low energy optically accessible state of the system and the two frequencies $\omega_1$ and $\omega_2$ have the same order of magnitude. Obviously (2) can then be written in the form:

$$\chi_i^{(2)} (-\omega_1 - \omega_2, \omega_1, \omega_2) = \frac{A_{SHG}}{\omega_{io} - (\omega_1 + \omega_2) + i\Gamma} \tag{3}$$

The electric field at $(\omega_1 + \omega_2)$ is obtained from Maxwell's equations and is proportional to $\chi^{(2)}$. The light intensity at $(\omega_1 + \omega_2)$ is then proportional to $|\chi^{(2)}|^2$. The damping parameter $\Gamma$ is the homogeneous linewidth for the resonant transition. In crystals and gases there is also inhomogeneous broadening, so the polarization becomes:

$$P(\omega_1 + \omega_2) = \int P_i(\omega_1 + \omega_2)\, g(\omega_{io} - \omega)\, d\omega \tag{4}$$

where $P_i$ is the polarization for the homogeneous system and $g(\omega_{io} - \omega)$ is the inhomogeneous distribution function peaking at $\omega_{io}$. In most of our experiments $\omega_1 = \omega_2$, and $g(\omega_{io} - \omega)$ is a gaussian distribution having a width parameter $\sigma$ so that the second harmonic light intensity near resonance is

$$I(2\omega_1) = K \left| A_{SHG} \int \frac{\exp[-(\omega_{io} - \omega)^2/\sigma^2]}{(\omega - 2\omega_1 + i\Gamma)}\, d\omega \right|^2 \tag{5}$$

where K depends on the phase matching (7). In most of our resonance experiments the system is perfectly phase matched at the peak signals. The resonance frequency $\omega_{io}$ corresponds to a polariton of particular wavevector, and in general the damping parameter is dependent on frequency for the case of polaritons (8). Apparently the factors in equation (3) or (5) will vanish unless the transition to the state i is both one and two photon electric dipole allowed, a situation that can prevail when the system is not centrosymmetric. For centrosymmetric systems (5) can exist if one of the three transition moments ($\mu_{oi}$, $\mu_{ij}$ or $\mu_{jo}$) is magnetic dipole (M) or electric quadrupole (9). The two situations that can arise are sketched in Figure 2. In Figure 2(a) the resonant state has the same parity as the ground state so the first factor in equation (3) is a magnetic dipole transition amplitude while the second is a normal two-photon amplitude involving intermediate states of u-parity. In Figure 2 (b) the resonant state has opposite parity from the ground state so the two-photon part of equation (3) contains the magnetic dipole transition moment. Both of these terms will be important in molecular spectroscopy. Case (a) will result in the production of coherent light at $\sim \omega_{oi}$ even in a conventional two-photon absorption experiment. Thus if the crystal has other transitions of the appropriate parity near $\omega_{oi}$ this beam may become absorbed in a secondary process, thereby resulting in a two-photon fluorescence signal. The anisotropy of two-photon transitions in crystals may therefore be subject to errors, since the two-photon absorption through Im $\{\chi^{(3)}\}$ does not have the same anisotropy as the effect discussed here. Case (b) gives rise to a coherent beam at $\sim \omega_{oi}$, and this beam can certainly be absorbed in a one photon process, since the $o \rightarrow i$ transition is allowed. If the two-photon transition is being detected by fluorescence or attenuation of the beams at $\omega_1$ or $\omega_2$ we see that the magnetic part of $|\chi^{(2)}|^2$ will contribute always in case (b) and also in case (a) if other u-states lie in the region of the state i. For the case (b) the

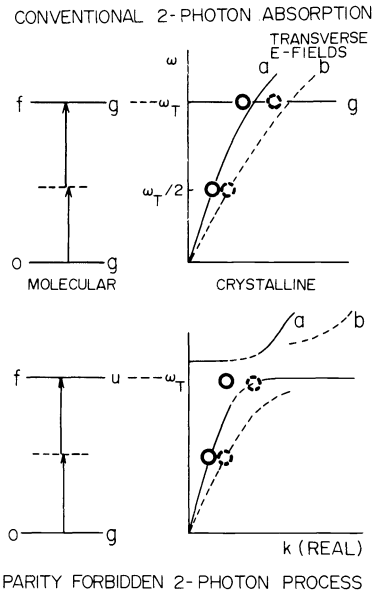


Figure 2. (a) Conventional allowed 2-photon processes.
(b) Unconventional forbidden 2-photon-process.
In (a) phase matching to produce excitons is non-critical; in (b) the phase matching is onto polariton states and it is critical.

separation of the second harmonic generation from two-photon absorption is not so simple to achieve experimentally. Far off resonance, where the attenuation of the second harmonic beam is small one may readily study the resonance enhanced SHG, but it is more difficult to separate the effects of SHG from two-photon absorption when an indirect method, such as fluorescence, is used to detect the two-photon transition. Ovbiously the same considerations will hold for systems having no center of symmetry. For example in a molecular crystal where the unit cell has no inversion center, the relaxed fluorescence resulting from two-photon resonances with vibronic states will contain resonant parts due to $|\chi^{(2)}|^2$ as well as Im $\{\chi^{(3)}\}$. One can therefore expect that two-photon induced fluorescence spectra would resemble closely the one-photon spectra of the same transitions, at least in the condensed phase. In general, molecules have states of different symmetry in the same spectral region because of the various vibrational or phonon symmetries. Thus radiation having a frequency larger than the 0-0 transition of a particular electronic state is always partially absorbed regardless of its polarization.

## 3. $\chi^{(2)}$ AND Im $\chi^{(3)}$ SPECTROSCOPY IN ORGANIC CRYSTALS:

In conventional induced two-photon processes connecting two stationary states of a crystal there is no phase matching difficulty. The situation, depicted in Figure 2(a), for a centrosymmetric system is that the Im $\{\chi^{(3)}\}$ describes two-photon absorption from the g - ground state to g - excited states of the crystal. Since electromagnetic fields at ca. $2\omega$ do not couple significantly to the system via the g → g transition the phase matching is entirely non-critical. For example (see Figure 2(a)) light having wavevector k and frequency $\omega$ matches to an exciton at $2\omega$ and 2k for all k. On the other hand (see Figure 2(b)) if the two-photon absorption is unconventional such as between a g and a u level of the crystal the "light" at $2\omega$ does interact with the crystal through the resonantly enhanced $\chi^{(1)}$ at $2\omega$. In that case the two-photon absorption is the fusion of two photon-polaritons to produce a polariton at ca. $2\omega$. Now the phase matching is critical since photons at $\omega$ phase match only for k=k'. Furthermore for optically nonisotropic crystals the observed spectrum will depend on the direction of propagation and polarization of the light at $\omega$, whereas in the conventional situation the spectral line position is the same for all directions of propagation. These same phase matching conditions should persist for two-photon absorption and second harmonic generation.

These features are illustrated by our recent work on the naphthalene crystal at low temperatures. Light at $\omega$ (region of $<6200$ Å) incident on the crystal produces many sharp transitions at $2\omega$ (region of $<3100$ Å) that were detected (10) by means of the fluorescence (incoherent emission) of the crystal. These two-photon spectra were independent of propagation direction in the crystal and the transitions were identified as $g \rightarrow g$ vibronic transitions corresponding to upper states involving the various ungerade vibrations of the naphthalene $B_{2u}$ state. In the region of $2\hbar\omega$ equal to the energy of the 0-0 band of this transition the situation is quite different (11). Here the two-photon absorption is dependent on the direction of propagation as shown in Figure 3. In addition to two-photon absorption in this experiment the second harmonic generation is observed for $2\omega$ both at lower and at higher energy than the region of two-photon absorption.

The spectrum of Figure 3 exposes the main features of the polariton dispersion curve. Of special interest is the knee region where the lower and upper branches come closest. When the phase matching is appropriate to reach the knee there should arise the possibility of widening the range of frequencies ($2\omega$) that can be reached with a given incident beam direction and laser divergence. In other words the phase matching curve at some direction of incidence will run parallel to the polariton dispersion curve. This appears to be a likely interpretation of the narrow angular region (marked near $-5^\circ$ in Figure 3) where the two photon induced signal is considerably broadened.

These spectra through their widths and the comparisons of second harmonic generation and two-photon absorption provide valuable information on the damping of polaritons in molecular crystals. The concepts involved in the dynamical aspects of excited states of crystals are illustrated in Figure 4.

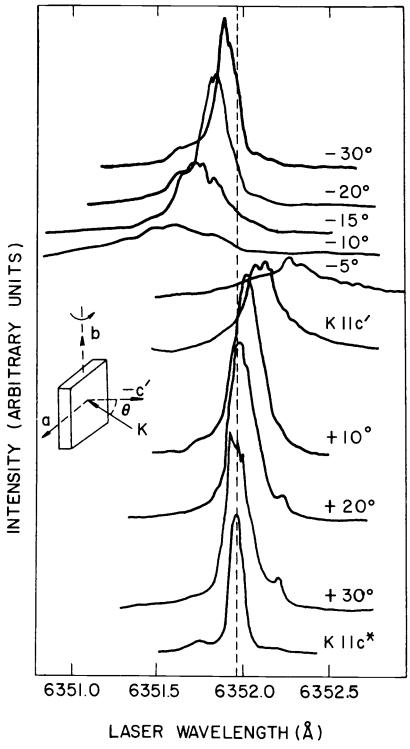


Figure 3. Two-photon excitation spectrum of naphthalene at 1.6K using colinear Geometry (11).

The distinction between coherent optical events in Figure 4 is quite analogous to the more conventional problem of distinguishing coherent scattering from incoherent fluorescence of molecular excited states (12). The field at $\omega$ if far from a crystal resonance propagates in the crystal as a photon-polariton. For weak fields in a perfect crystal this coherent polarization can only be diminished by conventional Raman scattering, creating new photon-

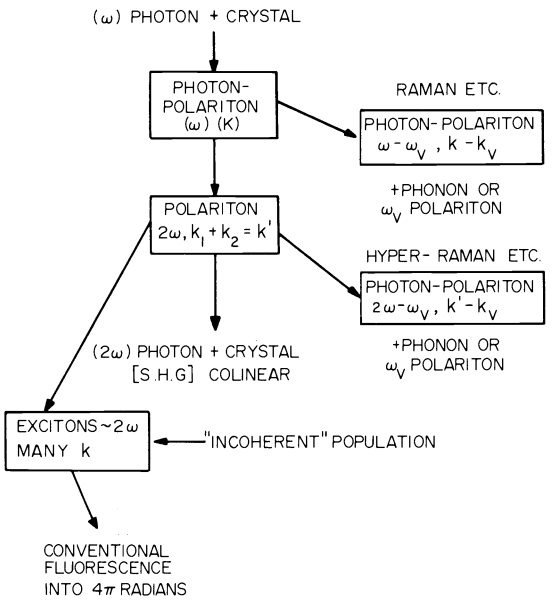


Figure 4. Dynamical events in light absorption by a crystal.

polaritons. The non-linear susceptibility allows polariton fusion to occur resulting in a coherent polarization at $2\omega$ and thus an electromagnetic field at $2\omega$ will be observed outside the crystal. When $2\omega$ is near a crystal resonance an exciton-polariton (or simply a polariton) is generated in the crystal. This polariton, which if undamped will result in the second harmonic wave, may be damped by various spontaneous processes. One way is the spontaneous production of a polariton and a phonon corresponding to different frequencies and wavevectors. This is hyper-Raman scattering. Another cause of damping is the exciton-phonon interaction which generates an incoherent population of excitons in the crystal. Clearly this damping depends on the exciton density of states at the polariton frequency. The population of excitons thus produced may radiate light in the region of $2\omega$ (or less) corresponding to conventional fluorescence of the crystal. This fluorescence is emitted into $4\pi$ radians with a spectral distribution given by the dephasing of the dipoles created in the crystal.

## 4. THREE-WAVE MIXING SPECTROSCOPY: GENERAL

In general two laser beams having frequencies $\omega_1$ and $\omega_2$ interact with a sample to produce a third beam, nearly colinear with the incident sources, that has a frequency $\omega_3 = 2\omega_1 - \omega_2$. It is very well known that the generation of the $\omega_3$ beam is strongly enhanced when $[\omega_1 - \omega_2]$ is also a vibrational (or electronic) frequency of the medium - this process being CARS. If the medium has a resonance at $2\omega_1$, an enhancement of the $\omega_3$ beam due to the two-photon resonance is also expected. Diagrams for these two resonances in $\chi^{(3)}$ are given in Figure 5.

Originally demonstrated (13) for excitons in CuCl the two-photon resonance has very recently been studied in organic liquids (14, 15). An advantage of the two-photon resonances in $\chi^{(3)}$ in studies of optical spectra is that comparisons of the CARS and two-photon resonant signals are readily achieved. The ratio of the two signals can be arranged in favorable circumstances to be independent of the power and mode structure of the lasers. The CARS portion involves only the Raman cross-section and linewidths.

If the $\omega_1$ beam is scanned and $\omega_2$ fixed, the intensity of the $\omega_3$ beam as a function of $\omega_1$ yields the spectrum of the resonances that occur at $2\omega_1$ when $(\omega_1 - \omega_2)$ is far from CARS resonances. The three wave mixing technique has great advantages over indirect methods of detecting two-photon absorption because no special properties of the resonant state are needed other than that a conventional two-photon matrix element exist between that state and the ground state. For example, two-photon resonances in three wave mixing could be studied for dissociative states and nonfluorescent systems whose lifetimes would preclude the use of the fluorescence methods of studying two-photon absorption. The spectral inten-

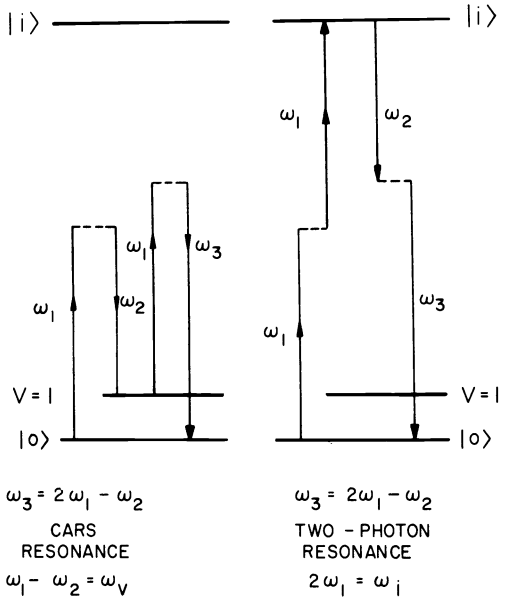


Figure 5. Two of the resonance processes involved in the generation of coherent light at $\omega_3$ due to the interaction of light at $\omega_1$ and $\omega_2$ with any medium.

sity profiles obtained are not influenced in a first approximation by higher order processes or by quantum yields of incoherent relaxations and so provide an unperturbed intensity distribution.

4. (a) TWO-PHOTON RESONANCES IN GASES (16):

Two-photon resonances in $\chi^{(3)}$ can be readily obtained for molecular gases and used for moderately high resolution spectroscopy. The well-known two-photon absorption spectrum of nitric oxide (17) was used in order to demonstrate the effects.

The experimental apparatus consisted of a Molectron UV1000 nitrogen laser used to pump two Hansch type dye lasers both of which produced 50 to 100 μj. The beams were rendered colinear through a 60° prism and focused into a 10 cm gas cell. Lenses were used after both lasers to partially compensate for divergence and to assure that both beams focused simultaneously in the same region. A prism monochromator and double 3/4m monochromator were used to select the $\omega_3 = 2\omega_1 - \omega_2$ beam, which was monitored by a Hamamatsu 213 photomultiplier tube. Signals were viewed on an oscilloscope in order to optimize detection, to confirm $\chi^{(3)}$ behavior that demands the signal intensity is proportional to $I_1^2 I_2$, and to remove scattered light problems. A Boxcar integrator was used as a linearly gated amplifier. Spectra were obtained by fixing $\omega_2$ at some desired frequency and scanning $\omega_1$ while the double monochromator was scanned at twice the $\omega_1$ rate. Monochromator bandpasses were kept as large as possible to minimize synchronization errors.

The two-photon resonances observed in NO (Figure 6) were easily identifiable by their invariance to the value of $\omega_2$, by their linewidths which were laser limited (the $\omega_1$ laser was narrower than the $\omega_2$ laser by at least a factor of 2), and by reference to known spectra.

The CARS resonance signals were observed for NO, and for $N_2$ in air after lifting the sample from the beam focus region. The latter signal was useful for maximizing detection optics before inserting the gas cell and searching for two-photon signals. Besides this helpful maximization, a calibration of the two-photon signal can be achieved since the cell alters the collection optics only minimally, and the CARS (Raman) resonance susceptibility for $N_2$ is known.

For a gas the damping parameter used in the expressions for the contribution of a

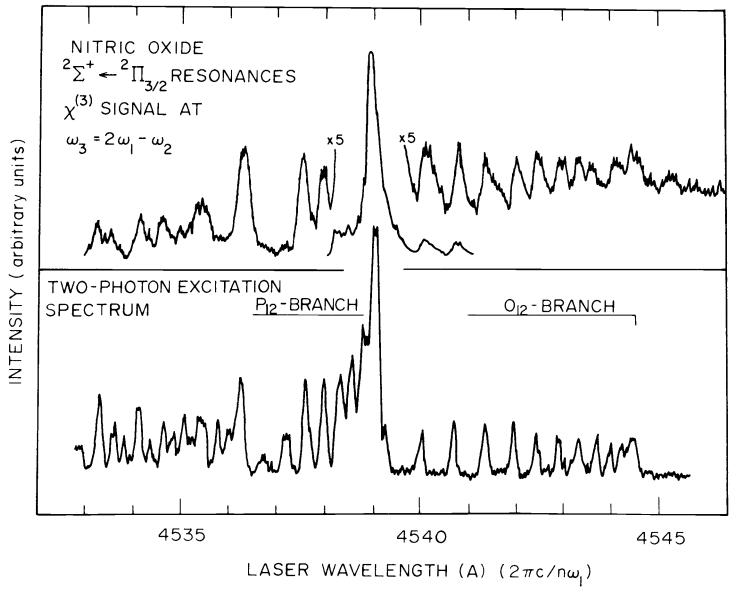


Figure 6. Two-photon resonances in NO gas.

resonance to $\chi^{(3)}$ is determined by the collisional and natural damping, and the Doppler broadening creates an inhomogeneous distribution of resonances. The nonlinear polarization at frequency $\omega$ is generated by the effect of the electric field amplitudes of all lasers operating through the bulk susceptibility function. That due to the $i^{th}$ resonance is

$$P_i(\omega) = \iiint d\omega_1' d\omega_1'' d\omega_2' \, \delta(\omega + \omega_2' - \omega_1' - \omega_1'') \, E_1(\omega_1')$$
$$E_1(\omega_1'') E_2(\omega_2') \int d\omega_i'' [\pi\sigma^2]^{-\frac{1}{2}} e^{-(\omega_i' - \omega_i)^2/\sigma^2} [2 - \delta_{\omega_i'\omega_j''}] 3 \chi_i^{(3)}(\omega_i', \Gamma_i) \quad (6)$$

where $\chi_i^{(3)}(\omega_1', \Gamma_i)$ is the susceptibility appropriate to a resonance at $\omega_i'$ with damping constant $\Gamma_i$, and $\sigma$ is the appropriate Doppler width. For the closely spaced J components of the nitrogen Raman Q-branch, the sum of these terms effectively yields the total polarization. The light intensity generated at $\omega$ is then proportional to the total polarization modulus squared.

The determination of two-photon cross sections relative to Raman cross sections have recently appeared in the literature (14, 15). Our laser widths were appreciably wider than the resonance widths, so the spectra must be deconvoluted. In addition, the homogeneous and inhomogeneous widths need to be known since the former enters the expression for $\chi^{(3)}$ at resonance and the latter describes the distribution of the resonances. The comparison to $N_2$ CARS in air is nevertheless a convenient way to calibrate the two-photon signal. The two-photon hyperpolarizability determined via this method, $|\alpha_{xx}^T \alpha_{yy}^T|$ for $E_1 \perp E_2, E_3$, is not that for two photons at $\omega_1$, but is the geometric mean of this cross section with that for absorption of two photons at frequencies $\omega_2$ and $\omega_3$ where $\omega_2 + \omega_3 = 2\omega_1$. In general $|\alpha_{xx}^T \alpha_{yy}^T|$ is different from the comparable quantity needed for two-photon cross-sections, say $|\alpha_{xx}^T|^2$, but in certain cases these averages are related.

By appropriate averaging we find for the $0_{12}$ branch of the $\gamma$ bands of NO that $|\alpha_{xx}^T \alpha_{yy}^T| = \frac{1}{2}|\alpha_{xx}^T|^2$. Our measurements yielded for $0_{12}(6\frac{1}{2})$, $|\alpha_{xx}^T|^2 = 3.0 \times 10^{-52}$ cm$^6$. The commonly quoted quantity $\delta$ for single beam two photon absorption in a single rotational transition is then

$$\delta = \frac{8\pi^3}{c^2} \omega^2 g(2\omega) \{|\alpha_{xx}^T|^2 / f[0_{12}(6\tfrac{1}{2})]\} f[J]$$

where g (2ω) is a normalized lineshape function, and the f [J] are line strengths from Table 2 of reference 18. Specifically for $0_{12}$ $(6\frac{1}{2})$ this yields

$$\delta = 7.5 \times 10^{-51} \text{ g } (2\bar{\nu}) \text{ cm}^4 \text{ s/photon-molecule with } \bar{\nu} \text{ in cm}^{-1}.$$

4. (b) TWO-PHOTON $\chi^{(3)}$ RESONANCES IN MOLECULAR SOLIDS (19):

In molecular crystals at low temperatures it is easily possible to separate spectrally transitions to the many different vibronic states. We have recently shown that $\chi^{(3)}$ spectroscopy can be used with great effect to study gerade resonant states in the ultraviolet by means of visible lasers (19).

One example we have studied is the biphenyl crystal. The first excited electronic state having the same spin as the ground state is $^1B_{3g}$, to which a two-photon transition from the ground state is fully allowed. The Raman spectrum of the biphenyl crystal is also well-known, and one of the strongest lines is at 1277 $cm^{-1}$. The demonstration of the $\chi^{(3)}$ spectroscopy of these two states ($^1B_{3g}$ electronic state and an $^1A_g$ vibrational state, the ground vibrational state being $^1A_g$) is shown in Figure 7.

In this experiment $\lambda_2 = 2\pi c/\omega_2$ was kept fixed at 6548 Å while $\omega_1$ was scanned through the regions where $\omega_1 - \omega_2$ equalled the vibrational frequency and $2\omega_1$ equalled the electronic resonance frequency. The general form of $\chi^{(3)}$ is

$$\chi^{(3)} = \frac{A_v}{\omega_v - (\omega_1 - \omega_2) + i\Gamma_v} + \frac{A_T}{\omega_E - 2\omega_1 + i\Gamma_E} + \chi^{NR} \qquad (7)$$

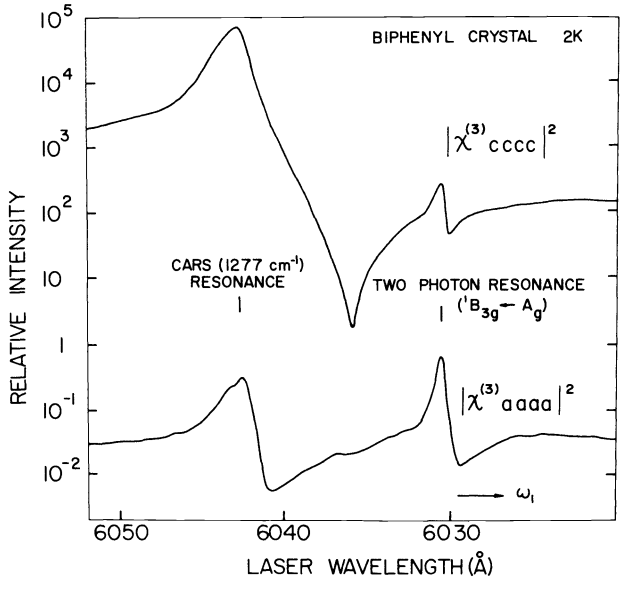


Figure 7. Two-photon and CARS resonances in the biphenyl crystal at 1.6K.

The $\omega_3$ signal shown in Figure 7, on scanning $\omega_1$ first goes through the vibrational (CARS) resonance, $(\omega_1 - \omega_2) = \omega_v$, and then the electronic resonance when $2\omega_1 = \omega_E$. The fact that the electronic state has different symmetry from the vibrational state is strongly manifested in Figure 7 by the entirely different anisotropies for three-wave mixing via the CARS and two-photon resonances.

5. THREE-PHOTON ABSORPTION:

The simultaneous absorption of three-photons to produce an incoherent population of excited states occurs through Im $\chi^{(5)}$ (see Figure 1). Whereas with many centrosymmetric organic crystals the two-photon absorption is an electronically forbidden process that requires the intervention of nuclear motion, those g → u transitions are allowed in three-photon ab-

sorption. Three-photon absorption is a useful adjunct to one-photon spectra in cases where XYZ belongs in a different irreducible representation than any of the three coordinates X, Y or Z. Such is the case with $D_{2h}$ where XYZ transforms as $A_u$. The benzene crystal factor group has symmetry $D_{2h}$ so that the molecular states are each split into four crystal states one of which has $A_u$ symmetry. Our preliminary study of the three-photon absorption is shown in Figure 8 (20).

This spectrum was seen by detecting fluorescence in the ultraviolet arising from absorption of three red photons from a single laser beam focused into a single crystal of benzene at 1.6K. The $A_u$ transition does not show up in this case because the electric vector is not projecting simultaneously onto all three crystal axes. The signal varies as $I_1^3$

## 6. TIME RESOLVED $\chi^{(3)}$ SPECTRA:

The various coherent spectroscopies described here are useful in studies of dynamics. For example in the nitric oxide experiments described above a 2ns laser pulse is used to probe the rotational temperature of NO. We have also used picosecond pulses to study the CARS resonance in nitrogen gas (21).

In gases the interval between hard sphere collisions is very long (ca $10^{-7}$ sec torr) compared with the duration of a picosecond pulse (say, 5 to 50 ps depending on the laser system used) even for relatively high pressures. Thus for vibrational effects, isolated molecule conditions might prevail up to many hundreds of torr when the experimental observations are made in the picosecond time regime. Rotational relaxation effects are known to have

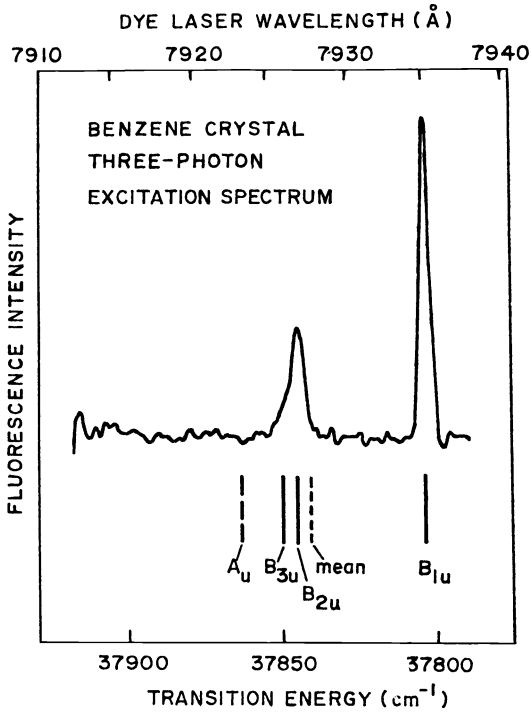


Figure 8. Three-photon excitation spectrum of crystalline benzene.

cross-sections often many times gas-kinetic, so the collision-free pressure limit relevant to picosecond experiments is not expected to be so high. Of course, except for rather light molecules the rotational spacings are in any case narrower than the transform frequency bandwidth of a picosecond pulse.

These experiments show the feasibility of using picosecond laser pulses to study ultrafast chemical reactions under essentially isolated molecule conditions at moderately high pressures. In many respects these non-linear phenomena are extremely convenient adjuncts to picosecond spectroscopy because they expand the range of wavelengths that can be used to study fast processes.

## 7. CONCLUSIONS:

The purpose of this presentation was to summarize some recent developments from this laboratory on applications of non-linear optical techniques in chemical spectroscopy. This field is very young and these early results suggest that non-linear optical spectroscopy at moderately high resolution will be a fruitful approach for the study of molecular excitons, mixed crystals and gases.

Acknowledgement - This research was supported by a PHS grant GM 12592, the Army Research Office (Durham), and the National Science Foundation, MRL Program under Grant No. DMR 76-00678.

REFERENCES:

1. N. Bloembergen, Nonlinear Optics, Benjamin, New York, 1965.
2. Y. R. Shen, Rev. Mod. Phys. 48, 1 (1976) and references contained therein.
3. D. Bedeaux and N. Bloembergen, Physica 69, 57 (1973).
4. C. Flytzanis, "Theory of Nonlinear Optical Susceptibilities" in Quantum Electronics: A Treatise, ed. H. Rabin and C. L. Tang, Academic, New York, 1975, Vol. I.
5. P. N. Butcher, Nonlinear Optical Phenomena, Ohio State University Engineering Publications, Columbus, 1965.
6. R. R. Birss, Symmetry and Magnetism, Selected Topics in Solid State Physics, Volume III; North-Holland 1966.
7. S. H. Kurtz, "Measurement of Nonlinear Optical Optical Susceptibilities" in Quantum Electronics: A Treatise, ed. H. Rabin and C. L. Tang, Academic, New York, 1975, Vol. I.
8. D. Frohlich, E. Mohler and Ch. Uihlein, Phys. Stat. Sol. 55, 175 (1973); D. Boggett and R. Loudon, J. Phys. C. 6, 1763 (1973).
9. S. Kielich, Acta Phys. Polon, 29, 875 (1965); P. S. Pershan, Phys. Rev. 130, 919 (1963).
10. R. M. Hochstrasser and H. N. Sung, J. Chem. Phys. 66, 3276 (1977).
11. R. M. Hochstrasser and G. R. Meredith, J. Chem. Phys. 67, 1273 (1977).
12. R. M. Hochstrasser and F. A. Novak, Chem. Phys. Lett., in Press.
13. S. D. Kramer, F. G. Parsons and N. Bloembergen, Phys. Rev. B 9, 1853 (1973); S D. Kramer and N. Bloembergen, Phys. Rev. B 14, 4654 (1976).
14. R. T. Lynch, Jr. and H. Lotem, J. Chem. Phys. 66, 1905 (1977).
15. R. J. M. Anderson, G. R. Holtom and Wm. M. McClain, J. Chem. Phys. 66, 3332 (1977).
16. R. M. Hochstrasser, G. R. Meredith and H. P. Trommsdorff, submitted to Chem. Phys. Lett.
17. R. G. Bray, R. M. Hochstrasser and J. E. Wessel, Chem. Phys. Lett., 27, 167 (1974); R. G. Bray, R. M. Hochstrasser and H. N. Sung, Chem. Phys. Lett. 33, 1 (1975).
18. R. G. Bray and R. M. Hochstrasser, Mol. Phys. 31, 1199 (1975).
19. R. M. Hochstrasser, G. R. Meredith and H. P. Trommsdorff, in preparation.
20. R. G. Bray, C. M. Klimcak and R. M. Hochstrasser, unpublished research from this laboratory.
21. B. Greene, R. M. Hochstrasser and R. B. Weisman (results illustrating picosecond CARS presented at the IUPAC symposium are in preparation for publication elsewhere.)